

# blood

2003 102: 3970-3979  
Prepublished online Aug 7, 2003;  
doi:10.1182/blood-2003-03-0977

## **A role for Rab27b in NF-E2-dependent pathways of platelet formation**

Sanjay Tiwari, Joseph E. Italiano, Jr, Duarte C. Barral, Emilie H. Mules, Edward K. Novak, Richard T. Swank, Miguel C. Seabra and Ramesh A. Shivdasani

---

Updated information and services can be found at:

<http://bloodjournal.hematologylibrary.org/cgi/content/full/102/12/3970>

Articles on similar topics may be found in the following *Blood* collections:

[Cytoskeleton](#) (142 articles)

[Signal Transduction](#) (1926 articles)

[Hematopoiesis](#) (2358 articles)

---

Information about reproducing this article in parts or in its entirety may be found online at:

[http://bloodjournal.hematologylibrary.org/misc/rights.dtl#repub\\_requests](http://bloodjournal.hematologylibrary.org/misc/rights.dtl#repub_requests)

Information about ordering reprints may be found online at:

<http://bloodjournal.hematologylibrary.org/misc/rights.dtl#reprints>

Information about subscriptions and ASH membership may be found online at:

<http://bloodjournal.hematologylibrary.org/subscriptions/index.dtl>

Blood (print ISSN 0006-4971, online ISSN 1528-0020), is published semimonthly by the American Society of Hematology, 1900 M St, NW, Suite 200, Washington DC 20036.  
Copyright 2007 by The American Society of Hematology; all rights reserved.



## A role for Rab27b in NF-E2-dependent pathways of platelet formation

Sanjay Tiwari, Joseph E. Italiano Jr, Duarte C. Barral, Emilie H. Mules, Edward K. Novak, Richard T. Swank, Miguel C. Seabra, and Ramesh A. Shivdasani

**Megakaryocytes release platelets by reorganizing the cytoplasm into proplatelet extensions. Fundamental to this process is the need to coordinate transport of products and organelles in the appropriate abundance to nascent platelets. The importance of the Rab family of small GTPases (guanosine 5'-triphosphatases) in platelet biogenesis is revealed in *gunmetal (gm/gm)* mice, which show deficient Rab isoprenylation and macrothrombocytopenia with few granules and abnormal megakaryocyte morphology. Although some Rab proteins are implicated**

**in vesicle and organelle transport along microtubules or actin, the role of any Rab protein in platelet biogenesis is unknown. The limited number of Rab proteins with defective membrane association in *gm/gm* megakaryocytes prominently includes Rab27a and Rab27b. Normal expression of Rab27b is especially increased with terminal megakaryocyte differentiation and dependent on nuclear factor-erythroid 2 (NF-E2), a transcription factor required for thrombopoiesis. Chromatin immunoprecipitation demonstrates recruitment of NF-E2 to the putative *Rab27B* promoter.**

**Inhibition of endogenous Rab27 function in primary megakaryocytes causes severe quantitative and qualitative defects in proplatelet formation that mimic findings in *gm/gm* cells. Rab27b localizes to alpha and dense granules in megakaryocytes. These results establish a role for Rab27 in platelet synthesis and suggest that Rab27b in particular may coordinate proplatelet formation with granule transport, possibly by recruiting specific effector pathways. (Blood. 2003;102:3970-3979)**

© 2003 by The American Society of Hematology

### Introduction

Mammalian blood platelets are released from bone marrow megakaryocytes (MKs) in a process that transforms the entire MK cytoplasm into long pseudopodia known as proplatelets.<sup>1-3</sup> Nascent platelets are assembled within these structures.<sup>4</sup> The need for dramatic cytoplasmic and cytoskeletal reorganization and concomitant assembly of anucleate platelets presents unusual challenges to differentiated MKs. The cellular and molecular response to these challenges is poorly understood.

Selected mouse models of thrombocytopenia and qualitative platelet defects have proved invaluable in probing the molecular basis of platelet biogenesis. Mice lacking either of 2 erythromegakaryocytic transcription factors, GATA1, and nuclear factor-erythroid 2 (NF-E2), show dramatically arrested MK maturation<sup>5,6</sup> and thus implicate their target genes in aspects of platelet assembly. However, the transcriptional targets of GATA1 and NF-E2 that are immediately relevant to MK fragmentation and platelet release are not known. Other insights derive from findings in animal models of the human Hermansky-Pudlak syndrome (HPS), a multigenic group of recessively inherited disorders that result from abnormal synthesis of 3 related organelles: melanosomes, platelet-dense granules, and lysosomes.<sup>7</sup> HPS proteins regulate intracellular vesicle traffic, including the  $\delta$  and  $\beta$ 3A subunits of the AP-3 adaptor complex, which captures organelle membrane proteins at the *trans*-Golgi apparatus and/or endosomes, and the pallid protein, which interacts with syntaxin-13 to mediate vesicle fusion.<sup>8,9</sup> These

HPS proteins highlight molecular pathways that serve to assemble and transport organelles but they do not overtly influence the efficiency with which MKs release platelets. In contrast, thrombocytopenia is a cardinal feature of the *gunmetal* mouse.<sup>10</sup> The cellular morphology of *gm/gm* MKs closely resembles that seen in the absence of NF-E2, with reduced numbers of  $\alpha$  and dense granules and disorganized internal membrane complexes.<sup>5,11</sup> Investigation of the reduced and defective platelet synthesis in *gunmetal* mice is thus especially suited to help elucidate thrombopoietic mechanisms.

The *gunmetal* mutation reduces cellular levels (to about 20% of normal) of the  $\alpha$  subunit of Rab geranylgeranyltransferase (RGGT),<sup>12</sup> the only enzyme known to attach lipid groups to the C-terminus of the Rab family of small Ras-like GTPases (guanosine 5'-triphosphatases). Covalent isoprenylation endows Rab proteins with lipophilic character and hence permits their association with target membranes.<sup>13</sup> Rab proteins constitute the largest family of Ras-related proteins, with more than 60 mammalian members that serve a vast array of functions involving internal membrane organelles.<sup>14,15</sup> However, the restricted phenotype of *gm/gm* mice indicates that selected cell types are overly susceptible to reduced RGGT levels; even though enzyme activity is equally diminished in all *gm/gm* tissues tested, the degree to which specific Rabs are affected varies by cell type.<sup>12,15,16</sup> Consistent with the *gm/gm* phenotype, significant deficits in isoprenylation are observed in

From the Departments of Medical Oncology and Cancer Biology, Dana-Farber Cancer Institute, Boston, MA; Departments of Medicine, Harvard Medical School and Brigham & Women's Hospital, Boston, MA; Cell and Molecular Biology, Division of Biomedical Sciences, Faculty of Medicine, Imperial College London, United Kingdom; and Roswell Park Cancer Institute, Buffalo, NY.

Submitted March 31, 2003; accepted July 31, 2003. Prepublished online as *Blood* First Edition Paper, August 7, 2003; DOI 10.1182/blood-2003-03-0977.

Supported by National Institutes of Health research grants R01HL63143, R01HL68130, R01HL51480, and R01EY12104, and the Medical Research

Council, United Kingdom. This research used core facilities supported in part by the National Cancer Institute-funded Center Support Grant CA16056. R.A.S. is a Scholar of the Leukemia and Lymphoma Society.

**Reprints:** Ramesh A. Shivdasani, Dana-Farber Cancer Institute, One Jimmy Fund Way, Boston, MA 02115; e-mail: ramesh\_shivdasani@dfci.harvard.edu.

The publication costs of this article were defrayed in part by page charge payment. Therefore, and solely to indicate this fact, this article is hereby marked "advertisement" in accordance with 18 U.S.C. section 1734.

© 2003 by The American Society of Hematology

melanocytes and platelets.<sup>16</sup> These lineage-restricted effects could result either from a high concentration of Rab proteins in target cells, so that reduced enzyme activity is limiting, or from the particular sensitivity of cell type-specific Rabs to reduced RGGT levels. Regardless of the precise mechanism, the *gunmetal* phenotype implies that efficient thrombopoiesis and granule biosynthesis rely on the degree of prenylation and membrane association of some Rab proteins.

Hypoprenylated Rab proteins in *gm/gm* tissues include the Rab27 subfamily,<sup>12</sup> which includes the products of 2 distinct genes, *Rab27A* and *Rab27B*, that share 71% amino acid sequence similarity.<sup>17,18</sup> *Rab27a* was originally cloned from an MK library and is widely expressed,<sup>17,19-21</sup> whereas *Rab27b*, also originally identified in platelets,<sup>19</sup> is virtually restricted in expression to platelets, the digestive tract, and the pituitary gland.<sup>17,18,21,22</sup> We investigated the roles of individual Rab proteins expressed in MKs and found that *Rab27b* fulfills many of the criteria expected of a Rab protein with a role in thrombopoiesis. Expression of *Rab27b* is greatly increased with terminal MK differentiation and is singular among MK-expressed Rabs for dependence on NF-E2. NF-E2 is recruited to the *Rab27b* promoter in differentiated MKs, representing experimental evidence for its direct regulation of a gene with a plausible role in thrombopoiesis. Inhibition of endogenous *Rab27* function in primary MKs causes severe quantitative and qualitative defects in proplatelet formation that recapitulate findings in *gunmetal* mutant mice. These observations provide new insights into the molecular and transcriptional regulation of platelet biogenesis.

## Materials and methods

### Plasmid constructs and antibodies

*Rab27b*, *Rab27bT23N*, *Rab27bN133I*, and *Rab7T22N* cDNAs were subcloned into the pEGFP-C1 or pEGFP-C3 vectors (Clontech, Palo Alto, CA); the resulting plasmids encode fusion proteins that contain each Rab protein or its corresponding mutant linked to the C-terminus of enhanced green fluorescent protein (EGFP).<sup>18,23,24</sup> Rabbit antisera against p45 NF-E2 were prepared as described previously<sup>25</sup> and immunoprecipitating p45 NF-E2 antibodies were kindly provided (Figure 4B) by Paul Ney (St Jude Children's Research Hospital, Memphis, TN) or purchased (Santa Cruz Biotechnology, Santa Cruz, CA; Figure 4D). Anti- $\beta$ 1 tubulin<sup>26</sup> and rabbit antimouse platelet<sup>27</sup> sera were generous gifts from Sally Lewis and Nick Cowan (New York University, New York, NY) and Carl Jackson (St Jude Children's Research Hospital), respectively. *Rab27b* antisera S086 was obtained and affinity purified as described previously<sup>21</sup> and antiserum R27B1 was raised against the *Rab27b* C-terminal peptide CKTQIPDVTNG-GNSG. Antisera N688 (recognizes both *Rab27* isoforms) and 4B12 (specific for *Rab27a*) were described previously.<sup>24</sup> Other antibodies were obtained from commercial sources: Transduction Laboratories (Lexington, KY) for Rab1b, Rab4, Rab6, and Rab8; Biodesign International (Kennebunk, ME) for GAPDH (glyceraldehyde 3-phosphate dehydrogenase); StressGen Biotechnologies (San Diego, CA) for calnexin; Diagnostica Stago (Asnières, France) for von Willebrand factor (VWF); and Abcam (Cambridge, United Kingdom) for the rat monoclonal antibody (Ab) against serotonin.

### Animal husbandry and megakaryocyte culture

The p45 NF-E2<sup>+/-</sup> (129/Sv strain), *gunmetal* (C57BL/6J-*gm/gm*), and *ashen* mice (C3H/HeSn-*ash/ash*) were maintained as described previously.<sup>5,11,21</sup> Wild-type littermates were used as controls in all experiments, thus ensuring control over strain-specific effects. Single-cell suspensions, obtained from fetal mouse livers between embryonic days 13 and 15 by repeated passage through 18- and 22-gauge needles, were cultured in Dulbecco modified Eagle medium (Life Technologies, Gaithersburg, MD)

supplemented with 10% fetal calf serum, 2 mM L-glutamine, 50 units/mL penicillin, 50  $\mu$ g/mL streptomycin, and 1% tissue culture supernatant from a murine c-Mpl ligand-producer cell line.<sup>25</sup> MK-enriched cell populations were isolated after a variable number of days in continuous culture by layering cell suspensions on a 1.5% to 3.0% albumin step gradient and sedimenting at 1g for 40 minutes. Proplatelet-producing MKs were scored manually by phase-contrast, fluorescence, or computer-assisted video microscopy on day 5 of suspension cultures. To evaluate Rab expression in relation to MK maturation, fetal liver cultures were separated over albumin density gradients on culture days 3, 4, or 6, when the predominant MKs are either immature (day 3), mature with a large cytoplasm but few if any proplatelets (day 4), or producing proplatelets in abundance (day 6).

### Subcellular fractionation and in vitro prenylation of cytosolic Rabs

Frozen MK, platelet, and leukocyte pellets were thawed, resuspended in lysis buffer (50 mM HEPES [N-2-hydroxyethylpiperazine-N'-2-ethanesulfonic acid], pH 7.2; 10 mM NaCl; 1 mM dithiothreitol [DTT]; 0.5 mM phenylmethylsulfonyl fluoride [PMSF]; 5  $\mu$ g/mL pepstatin; 5  $\mu$ g/mL aprotinin; and 5  $\mu$ g/mL leupeptin) and mechanically disrupted by passages through a 21-gauge needle. For subcellular fractionation, the MK homogenates were first centrifuged at 1000g for 10 minutes at 4°C to obtain the postnuclear supernatant (PNS). The PNS was then centrifuged at 100 000g for 1 hour at 4°C and the supernatant (S<sub>100</sub>) saved. The pellet (P<sub>100</sub>) was resuspended in the same volume of lysis buffer and protein concentration in the PNS determined using Coomassie Plus reagent (Pierce, Rockford, IL). For the in vitro prenylation the cytosolic fractions (S<sub>100</sub>) of MK, platelets and leukocytes were used. Sixteen micrograms of *gm/gm*, *+gm*, or *+/+* cytosolic protein was added to 25- $\mu$ L reactions containing 50 mM HEPES, pH 7.2; 5 mM MgCl<sub>2</sub>; 1 mM DTT; 50  $\mu$ M NP-40 (nonidet P-40); 1  $\mu$ M [<sup>3</sup>H] geranylgeranyl pyrophosphate, 47 300 disintegrations per minute (dpm)/pmol; and 0.5  $\mu$ M each of recombinant RGGT and Rab escort protein 1 (REP-1). After incubation for 30 minutes at 37°C, samples were resolved in 17.5% polyacrylamide and visualized by autoradiography.

### Semiquantitative RT-PCR

Total cellular RNA was isolated from purified MKs using RNeasy RLT (Qiagen, Crawfordsville, IN) and reverse transcribed using oligo-dT primer. Reverse transcriptase-polymerase chain reaction (RT-PCR) was performed for cycle numbers in the linear range of amplification using  $\alpha$ [<sup>32</sup>P]dCTP (deoxycytosine triphosphate) as a radiotracer. The following primers were used at the annealing temperature of 58°C: Rab4 (5'-GAGCGGTTCAGGCTGTGACG3' and 5'-GAGCCTGTGTACGTCGAGGTG 3'), Rab6 (5'-GAGCAGAGCGTTGAAAGACG3' and 5'-GCCGCTTCATTGACTGGTTG3'), Rab8 (5'-GTCCTGTTCCGCTTCTCCGAG3' and 5'-GCTGGTCTCTTCTGCTGCTC3'), *Rab27a* (5'-TGTCGGA-TGGAGATTACGATTACC3' and 5'-CAGCACTGGTTTCAAAT-AGGGG3'), and *Rab27b* (5'-GCCCTCCAAGACCATCACTATG3' and 5'-GCTCCATCTGCTCCTTGTGTGT3').

### Chromatin immunoprecipitation (ChIP)

ChIP assays were performed as described previously,<sup>28</sup> with minor modifications. Cells isolated from the livers of 14.5 days after coitus (dpc) mouse embryos were cultured in the presence of thrombopoietin for 4 days, as described in "Animal husbandry and megakaryocyte culture." An MK-enriched cell population was isolated and cross-linked with formaldehyde at a final concentration of 0.4% for 10 minutes at ambient temperature with gentle agitation. Glycine (0.125 M) was added to quench the reaction and the cells were pelleted at 800g for 5 minutes and washed in phosphate-buffered saline (PBS). Nuclei were isolated by incubation in lysis buffer (10 mM Tris [tris(hydroxymethyl)aminomethane], pH 8.0; 10 mM NaCl; 0.2% Nonidet P-40; 1  $\mu$ g/mL leupeptin; 50  $\mu$ g/mL PMSF) on ice for 10 minutes, followed by centrifugation at 1800g for 5 minutes. Nuclei were lysed in 0.3 mL lysis buffer (50 mM Tris, pH 8.1; 10 mM EDTA [ethylenediaminetetraacetic acid], 1% SDS [sodium dodecyl sulfate]) for 10 minutes on ice. The lysate was sonicated 3  $\times$  15 seconds at a setting of 30 with a sonicator

(Fisher model 300; Fisher Scientific, Pittsburgh, PA) equipped with a microtip to shear chromatin fragments. The chromatin was diluted 4-fold in dilution buffer (20 mM Tris, pH 8.1; 150 mM NaCl; 2 mM EDTA; 0.01% SDS; 1% Triton X-100; 1  $\mu$ g/mL leupeptin; 50  $\mu$ g/mL PMSF) and precleared with 25  $\mu$ L preimmune serum followed by 50  $\mu$ L protein A–sepharose. The supernatant was collected and an aliquot removed (input) for subsequent PCR analysis. The remaining chromatin was divided in equal volumes for further incubation with 15  $\mu$ L of anti-p45 or preimmune serum for 3 hours at 4°C followed by 30  $\mu$ L of protein A–sepharose for 1 hour. A molar excess of competitor peptides were included in some experiments. Sepharose beads were harvested by centrifugation and washed, and DNA was isolated for PCR as described.<sup>28</sup> Primers used for PCR (5' to 3') included the following: Rab27bNFE2A (GGAAGTCCTT-GCTCTAGGAG and CTGATCGATCGTTGCAAGGC), Rab27bNFE2B (GGATGCTAGCTGATGAAGTCTG and AGTCTGCAGAGAGAGCCACATC), Rab27bNFE2C (GAGCTGTGGATAAGACCAGG and CTAGGTATTCGCAACTAGCC), Rab27bNFE2D (AGCCACTGTGTCAGCTGCAG and CTCATAGCTACAGGACAGC), Rab27bNFE2UP (GGAGAGCAGAGGTGATCTAG and CAGAGCCACAAGGCAAGTCA), Rab27bNFE2DN (CACGTGGTTTCAGGTTGACATC and CAGAACCTCCACTCCATACTG), Rab8NFE2A (CAGGACCTCTGGAAAGATCAG and CGCCGGTAGGGCTATGTTAT), Rab8NFE2B/C (CTGACAGATGTGTACTGCCAC and GTAGTAGCAAAGGTCTGCTG), and Rab8NFE2D (CCATGCTCCTGTGACTAAGTC and CCATGATAGGCAAGAGATGGC). PCR products were quantified by analysis of ethidium bromide–stained gels using National Institutes of Health (NIH) Image 1.61 software (<http://rsb.info.nih.gov/nih-image>).

### Immunoblot analysis

Immunoblots were performed according to standard protocols.<sup>29</sup> Cell extracts were resolved by SDS–polyacrylamide gel electrophoresis (SDS-PAGE) and transferred to polyvinylidene fluoride (PVDF) membranes. All primary antibodies, except affinity-purified S086, were incubated at 1:1000 dilution. After 3 washes, membranes were incubated with 1:10 000 dilution of horseradish peroxidase (HRP)–conjugated goat antirabbit immunoglobulin G (IgG; Santa Cruz Biotechnology) or 1:2500 dilution for HRP-conjugated goat antimouse IgG (Amersham, Arlington Heights, IL) for 1 hour and washed again. Signals were detected using enzymatic chemiluminescence (Amersham) and, where shown, quantified by analysis of band intensity using NIH Image 1.61 software.

### Megakaryocyte transfection

Cells derived from mouse fetal livers cultured in the presence of thrombopoietin, as described above, were harvested after 2.5 days. Plasmids encoding fusion products between EGFP and wild-type or mutant Rab proteins, driven by the cytomegalovirus (CMV) promoter, were coated onto 0.6- $\mu$ m gold beads by the method of Sanford et al.<sup>30</sup> The gold beads (10 mg) were suspended in 70% ethanol, washed with distilled water, and suspended in 50% (vol/vol) glycerol to a final concentration of 60 mg/mL. Ten microliters of bead slurry was then incubated with 1  $\mu$ g plasmid, 10  $\mu$ L of 2.5 M CaCl<sub>2</sub>, and 4  $\mu$ L of 0.1 M spermidine with continuous vortexing for 3 minutes. The gold was pelleted by pulse microcentrifugation, washed sequentially with 70% and 100% ethanol, and resuspended in 100  $\mu$ L of 100% ethanol. Ten microliters of the DNA-coated beads was placed on a macrocarrier and delivered into cells spread in a 10- $\mu$ L volume in the center of a 35-mm tissue-culture dish. This was achieved at a pressure of 900 psi at 10 mm Hg using a power density spectrum (PDS) 1000 He Biolistic particle delivery system (Bio-Rad, Hercules, CA) and resulted in transduction efficiencies between 0.5% and 1%. Cells were returned to culture for 24 hours before analysis for proplatelet formation or immunostaining for VWF.

### Immunofluorescence

Transfected megakaryocytes were cytocentrifuged gently onto poly-L-lysine-coated glass slides, fixed in 4% paraformaldehyde in PBS for 20 minutes, and incubated with 5% goat serum in 0.05% saponin in PBS for 30 minutes. Cellular autofluorescence was quenched by two 5-minute treatments with 1 mg/mL sodium borohydride (NaBH<sub>4</sub>) freshly prepared in PBS. Rabbit

anti-VWF serum (Diagnostica Stago) was added at 1:200 dilution in 1% goat serum containing 0.05% saponin in PBS and incubated at ambient temperature for 30 minutes. After washing in PBS, cells were treated with Texas Red–conjugated antirabbit IgG (Jackson ImmunoResearch, West Grove, PA) at 1:400 dilution in 0.05% saponin in PBS for 30 minutes. Staining controls were processed identically except for omission of the primary antibody. Preparations were observed using a Zeiss Axioskop 2 microscope ( $\times$  40 oil objective; Thornwood, NY) equipped with appropriate filters for GFP and Texas Red fluorescence emission. In colocalization experiments, antiserum R27B1 was conjugated directly with fluorescein isothiocyanate (FITC) and the rabbit anti-VWF serum was conjugated directly to Texas Red. Cells were observed with a Bio-Rad MRC 1024 laser scanning confocal microscope ( $\times$  100 Differential Interference Contrast-Apochromatic oil immersion objective).

## Results

### A requirement for Rab function in proplatelet formation

Previous studies suggest that the thrombocytopenia in *gm/gm* mice results from reduced production rather than excessive destruction of blood platelets.<sup>10</sup> To investigate the cellular basis for this deficit, we studied proplatelet formation by MKs cultured in the presence of thrombopoietin (Tpo).<sup>31</sup> Compared with *+gm* controls, the proportion of *gm/gm* MKs elaborating proplatelets at any time is reduced approximately 10-fold, as judged by phase-contrast microscopy (Figure 1A), and their proplatelets harbor notable qualitative defects. The *gm/gm* MKs usually form early, blunt pseudopodia that fail to convert into the typically long, beaded proplatelet extensions (Figure 1B). Immunofluorescent staining for  $\beta$ 1 tubulin, a sensitive marker of MK maturation,<sup>32</sup> reveals poorly developed proplatelet extensions in many fewer *gm/gm* MKs than in control cells (Figure 1C–D), despite normal  $\beta$ 1 tubulin protein levels (Figure 1E), and the constrictions that separate platelet-sized areas along the proplatelet shaft are reduced or absent. The observed reduction in proplatelet numbers does not follow trivially from a decrease in MK proliferation or reflect a substantial early block in MK differentiation, as MK progenitor numbers are normal and the DNA ploidy profiles of *+gm* and *gm/gm* MKs are nearly identical (data not shown). Indeed, because thrombocytopenia in *gm/gm* mice is associated with a compensatory 4-fold increase in MK numbers,<sup>11</sup> the approximately 10-fold reduction in proplatelet formation correlates well with the 50% reduction in circulating platelets and implicates the proplatelet formation defects in producing fewer platelets *in vivo*.

### Defining the molecular defects in *gm/gm* MKs

RGGT enzyme activity is reduced to about 20% of normal levels in *gm/gm* mice; this impairs prenylation of Rab proteins and compromises their function.<sup>12</sup> However, the activity of only a portion of the more than 60 known Rab proteins appears to be sensitive to this enzymatic deficiency, as the phenotype of *gm/gm* mice is limited to hypopigmentation and thrombocytopenia. To define the molecular basis for MK defects in *gm/gm* mice, we performed *in vitro* prenylation assays on MK and platelet cytosolic extracts in the presence of recombinant RGGT and Rab escort protein 1 (REP-1).<sup>20,33</sup> In this assay, unprenylated Rab proteins are modified by covalent addition of [<sup>3</sup>H]geranylgeranyl pyrophosphate and detected by autoradiography after SDS-PAGE. The *+gm* lysates contain no radiolabeled bands, confirming that cellular Rabs are efficiently prenylated in normal blood cells, whereas *gm/gm* lysates show a limited number of hypoprenylated Rab proteins (Figure

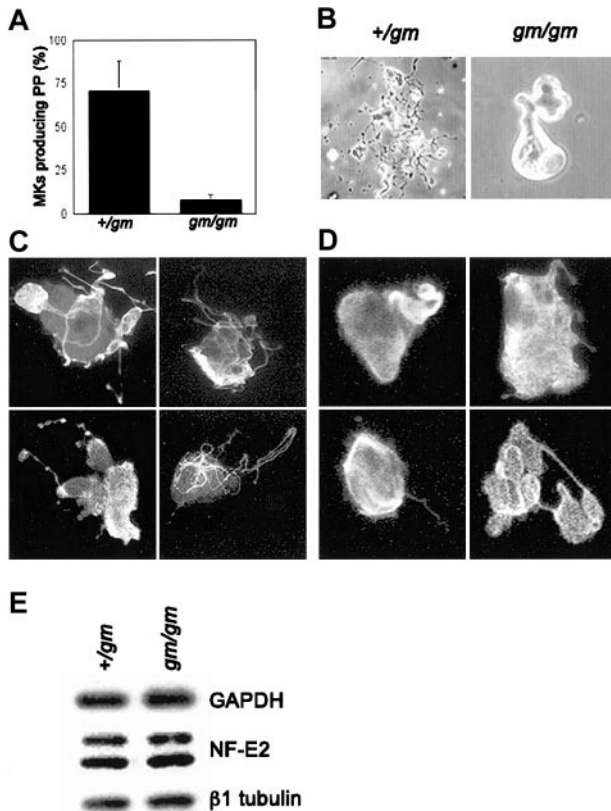


**Figure 1. Proplatelet formation defects in *gm/gm* MKs.** (A) Proplatelet formation is reduced approximately 10-fold in *gm/gm* MKs. Mouse fetal liver cells were cultured in thrombopoietin for 4 days before isolation of MKs that were analyzed for proplatelet formation the following day by phase-contrast microscopy. The percentage of proplatelet (PP)-producing MKs is expressed as mean  $\pm$  SD. (B) Phase-contrast micrographs of representative *+/gm* and *gm/gm* cells on culture day 5. The *+/gm* MKs elaborate rich proplatelet networks, whereas *gm/gm* MKs only form a few blunt pseudopodia. (C-D) Immunofluorescent detection of  $\beta$ 1 tubulin in cultured *+/gm* (C) and *gm/gm* (D) MKs. The increased sensitivity of this assay reveals that *gm/gm* MKs initiate proplatelet formation but the cytoplasmic extensions develop and elongate poorly. Original magnifications,  $\times$  400. (E) Immunoblot analysis of cultured *+/gm* and *gm/gm* MKs showing normal levels of  $\beta$ 1 tubulin and p45 NF-E2. Glyceraldehyde 3-phosphate dehydrogenase (GAPDH) is used as a loading control.

2A). The electrophoretic pattern of labeled *gm/gm* Rabs is superficially similar in leukocytes and MKs or platelets. However, the slowest migrating protein constitutes a greater fraction of the Rab proteins in platelets than in MKs, suggesting that it is either preferentially incorporated in platelets or a particularly late product in MK differentiation. A previous study showed that a similar slow-migrating Rab protein in lymphocytes was a member of the Rab27 subfamily,<sup>33</sup> and in subcellular fractionation experiments both Rab27a and Rab27b are found exclusively in the soluble, nonmembrane fraction of *gm/gm* MKs, attesting to their hypoprenylation (Figure 2B). Furthermore, the level of Rab27b is reduced in *gm/gm* MKs, as revealed in both the soluble and postnuclear supernatant fractions (Figure 2B).

The mouse coat color mutant *ashen* is due to a splice site mutation that abolishes Rab27a expression.<sup>34</sup> The *ash/ash* mice have normal platelet numbers<sup>21</sup> and examination of their MKs reveals no compromise in elaboration of proplatelets (data not shown). To determine the relative abundance of the 2 Rab27 isoforms, we performed immunoblot analysis of MK lysates using specific antibodies. Despite absence of Rab27a, total Rab27 protein levels in *ash/ash* lysates are similar to those in control cells, suggesting that Rab27b is the predominant isoform expressed in MKs (Figure 2C). Six Rab proteins are present at appreciable levels in blood platelets.<sup>35</sup> Among these, the amount of

Rab27b increases the most significantly ( $> 8$ -fold) and earliest in the maturation process, in contrast to Rab27a and other Rabs whose changes in expression are both more modest (1.2- to 4-fold) and slower (Figure 2D).

Taken together, these results point to (1) abundant expression of Rab27b in MKs and platelets, especially relative to Rab27a; (2) the possibility that reduced Rab27b activity in the *gm/gm* mouse contributes to its platelet defect; and (3) absence of a requirement for Rab27a in thrombopoiesis. These observations led us to suspect that Rab27b may play some role in platelet production.

#### MK expression of Rab27b depends on the transcription factor NF-E2

Like the *gunmetal* mutant, mice lacking the transcription factor NF-E2 are profoundly thrombocytopenic as a result of failure to form proplatelets.<sup>5,31,36</sup> Moreover, MKs in both mouse mutants display the common features of disorganized demarcation membranes and reduced

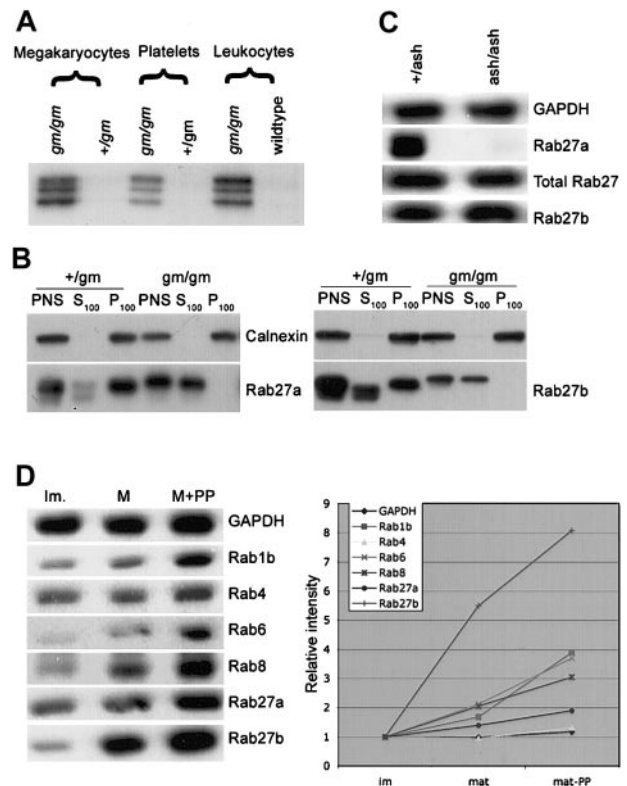


**Figure 2. Rab27b is hypoprenylated in *gm/gm* MKs and expressed abundantly in late stages of normal MK maturation.** (A) In vitro prenylation assay shows that a limited number of Rab proteins is hypoprenylated in *gm/gm* MKs. Cytosolic lysates were incubated in the presence of recombinant RGGT, Rab escort protein 1 (REP-1), and [<sup>3</sup>H]geranylgeranyl pyrophosphate as the lipid donor, followed by gel electrophoresis and autoradiography. (B) Immunoblot of postnuclear supernatant extracts (PNS; 25  $\mu$ g) or the soluble (S<sub>100</sub>) and membrane-associated (P<sub>100</sub>) fractions from *+/gm* and *gm/gm* MKs using Rab27a (4B12), Rab27b (S086), or calnexin (loading control) antibodies. The results indicate hypoprenylation of Rab27a and Rab27b in *gm/gm* MKs. (C) Immunoblot analysis of *+/ash* and *ash/ash* MKs using 4B12, R27B1 (anti-Rab27b), or an antibody (N688) that reacts with both Rab27a and Rab27b. Total Rab27 levels in *ash/ash* MKs are similar to control cells despite absence of Rab27a; this implies that Rab27b is the predominant subfamily member present in maturing MKs. (D) Immunoblot of MK cell populations enriched for different stages of maturation (Im indicates immature MKs on fetal liver culture day 3; M, mature MKs with few or no proplatelets on culture day 4; and M+PP, predominantly terminally differentiated proplatelet-producing MKs on culture day 6) with antibodies specific for known platelet-expressed Rab proteins or GAPDH. Relative levels of the chemiluminescence signal were quantified digitally and are represented in the right panel. Levels of Rab27b increase the most dramatically with MK maturation and proplatelet formation.

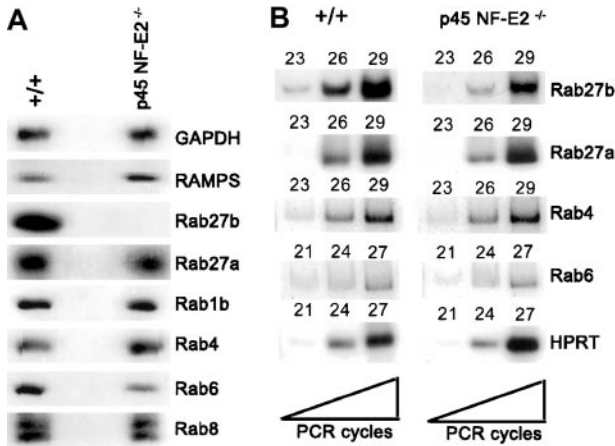


**Figure 3. Rab27b is absent in p45 NF-E2<sup>-/-</sup> MKs.** (A) Immunoblot of wild-type and p45 NF-E2<sup>-/-</sup> MKs using antibodies specific for the 6 Rab proteins known to be expressed in blood platelets or GAPDH and rabbit antimouse platelet serum (RAMPS) as loading controls. (B) Semiquantitative RT-PCR analysis shows Rab27b mRNA levels to be significantly reduced in the absence of NF-E2 function. The cDNA was synthesized from wild-type and p45 NF-E2<sup>-/-</sup> MKs isolated over an albumin density gradient and amplified by PCR in the presence of  $\alpha$ -[<sup>32</sup>P]dCTP radiotracer using primers specific for each Rab gene or for hypoxanthine phosphoribosyl transferase (HPRT). The number of PCR cycles was varied as indicated, and products were visualized by autoradiography. Results of both RT-PCR and immunoblot analysis are representative of 3 independent experiments.

numbers of dense and  $\alpha$  granules.<sup>5,10</sup> To test the possibility that the shared phenotypes in part reflect common molecular deficits, we examined the levels in p45 NF-E2<sup>-/-</sup> MKs of each of the 6 Rab proteins known to be expressed in the MK-platelet lineage.<sup>35</sup> Rab27b is completely absent from these cells (Figure 3A), whereas other Rabs are present at nearly normal levels. Hence, the *gm/gm* and p45 NF-E2 mutants represent independent mouse lines in which thrombopoietic deficits are associated with loss of functional Rab27b. However, absence of NF-E2 is associated with many defects besides loss of Rab27b expression.<sup>32,37-39</sup>

Despite the central importance of NF-E2 in platelet release, its critical transcriptional targets in MKs are largely unknown. The absence of Rab27b from p45 NF-E2<sup>-/-</sup> MKs raises the possibility that it may represent one such target. Indeed, in contrast to each of the other tested Rabs, steady-state levels of Rab27b mRNA are reduced about 8-fold in p45 NF-E2<sup>-/-</sup> MKs compared with control cells (Figure 3B; a signal appears after only 23 cycles of RT-PCR in wild-type cells, whereas a signal of lower intensity appears after 26 cycles in NF-E2-deficient MKs). Thus, the reduced Rab27b protein levels likely reflect lower levels of gene transcription.

Analysis of the murine *Rab27b* gene locus<sup>18</sup> identifies 4 potential NF-E2 binding sites (designated A-D in Figure 4A) between 1 kb upstream of the transcription start site and the end of the large first intron. Chromatin immunoprecipitation (ChIP) is a proven and useful approach to assess transcriptional regulation by NF-E2 and other factors in many contexts<sup>40,41</sup> and we used this method to determine if NF-E2 is recruited to any of its putative binding sites in the *Rab27b* locus. To establish specificity in this PCR-based assay, we first performed ChIP using dimethyl sulfoxide (DMSO)-treated murine erythroleukemia (MEL) cells, which activate NF-E2-dependent  $\beta$ -globin gene expression, and PCR primers specific for DNase I hypersensitive site 2 (HS2) within the  $\beta$ -globin locus control region.<sup>42-44</sup> Immunoprecipitation with anti-p45 NF-E2 antibody recovered HS2 fragments efficiently and selectively from the erythroid-enriched, MK-depleted cell fraction; induction with DMSO increased this capture (data not shown). In cultured cell fractions enriched for MKs, p45 NF-E2 antiserum consistently recovers the Rab27b NF-E2(A) fragment (Figure 4B). The fragments designated B-D are never recovered in the same experiments, whereas recovery of fragment A is competed in the presence of excess peptide antigen (Figure 4B) and reproduced with an independent p45 NF-E2 antibody (Figure 4D). To evaluate the specificity of these findings, we probed p45 NF-E2 chromatin immunoprecipitates for the presence of DNA fragments from additional regions: 2 areas approximately 2 kb on either side of the A site in the *Rab27b* locus (to further confirm specificity *in cis*) and 3 others from the promoter and first intron of the murine *Rab8* locus, which also contains 4 potential NF-E2 binding sites (Figure

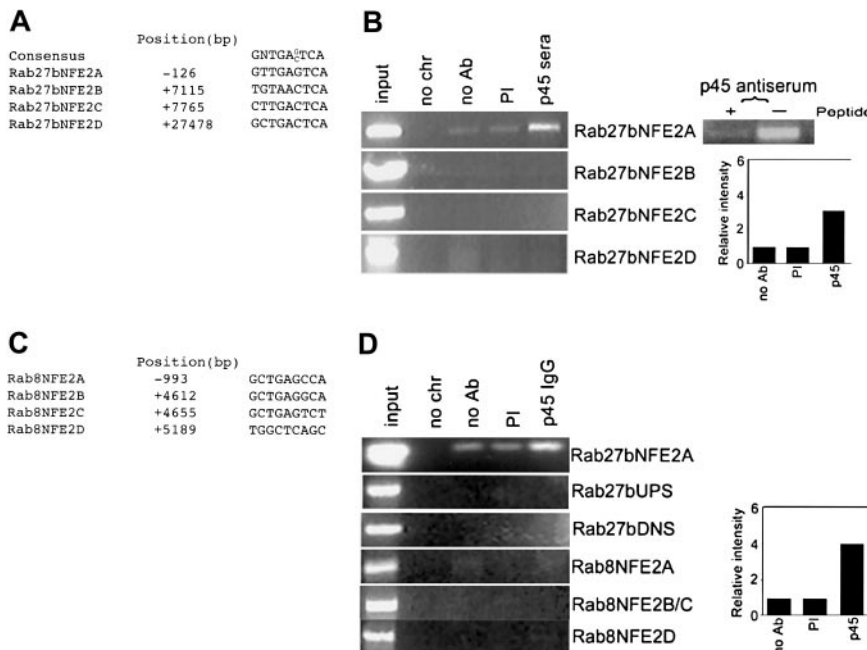


**Figure 4. Rab27b may be a direct transcriptional target of NF-E2.** (A) Four potential NF-E2 binding sites, here designated A-D, are identified between 1 kb upstream of the transcription start site (designated position +1) and the end of the first intron in the mouse *Rab27b* gene locus, using software that detects consensus matches in nucleotide sequence (<http://www.genomatix.de/matinspector>). (B) Chromatin immunoprecipitation (ChIP) analysis of primary MKs using p45 NF-E2 antibody indicates that NF-E2 is recruited to the A site of the *Rab27b* locus. PCR products were detected on ethidium bromide-stained agarose gels. Immunoprecipitating antibodies and conditions are indicated as follows: no chr indicates no chromatin; no Ab, none; p45, rabbit p45 NF-E2 antiserum; and PI, preimmune serum. The adjacent panels show an additional control with absence or presence of excess peptide antigen as a competitor in the immunoprecipitation and a histogram of quantitation of the visible bands in units of relative pixel density. The results shown are representative of 5 independent experiments. (C) Sequence and location of 4 potential NF-E2 binding sites, designated A-D, identified between 1 kb upstream of the transcription start site (designated +1) and the end of the first intron in the mouse *Rab8* gene. (D) ChIP analysis of primary MKs using a different p45 NF-E2 antibody verifies that NF-E2 is recruited to the A site in the *Rab27b* promoter (quantified in the right panel) but not 2 kb upstream (Rab27bNFE2UP) or downstream (Rab27bNFE2DNS) in the locus or to potential sites in the *Rab8* gene.

4C). None of these regions could be amplified under conditions in which the Rab27b NF-E2(A) site was detected readily (Figure 4D). Taken together, these results imply that NF-E2 associates with the *Rab27b* locus through at least one binding site in the putative promoter, and they suggest a direct role for NF-E2 in activating *Rab27b* gene transcription in MKs.

#### Function of Rab27b in MK fragmentation

The 10-fold lower proplatelet formation by *gm/gm* MKs indicates that one or more Rab proteins is required in this process, and the foregoing analysis points to Rab27b as a likely important component. To investigate Rab27b function in proplatelet formation, we transfected wild-type MKs with GFP-tagged dominant inhibitory versions of Rab27b (N133I and T23N, which correspond to the dominant-negative RasN116I and RasS17N, respectively<sup>24</sup>) and assessed proplatelet formation the next day. These constructs are well validated in the literature<sup>22,24,33</sup> and we confirmed the activity in a Rab GTPase assay in vitro (data not shown). We transduced primary MKs on culture day 2.5 because at later stages cells become excessively fragile and sustain damage on the transduction protocol. The starting cell population is consequently relatively immature and proplatelet formation is inefficient, even in untransfected controls (24% ± 2.5%), relative to unmanipulated wild-type MKs (eg, Figure 1A) but is not significantly attenuated (16% ± 2%) in mock-transfected cells (Figure 5A). MKs expressing either of the 2 dominant inhibitory constructs show about a 5-fold reduced proplatelet formation (Figure 5A), as defined by the presence of 2 or more pseudopodial cytoplasmic extensions, compared with cells transfected with wild-type Rab27b. Significantly, the cytoplasmic extensions formed by MKs expressing dominant-negative Rab27 forms are consistently much shorter than those seen in control-transfected cells (Figure 5B). This combination of findings resembles both major defects revealed in our cellular analysis of *gm/gm* MKs.

Overexpression of the N133I or T23N mutants is likely to interrupt recycling of the native protein by depleting Rab-specific GTP-exchange factors. To substantiate that the effects on proplatelet formation result from specific inactivation of endogenous Rab27 proteins, we overexpressed the Rab27 binding domain of synaptotagmin-like protein-1 (Slp1), a Rab27 effector.<sup>45,46</sup> Transient expression of GFP-tagged Slp1(1-150) in melanocytes has a demonstrated antagonistic effect by perturbing association of Rab27 with its endogenous effectors.<sup>45</sup> MK expression of GFP-tagged Slp1(1-150) also results in reduced numbers of MKs that elaborate bona fide proplatelets, at a magnitude comparable to that observed with the N133I or T23N mutants, and individual proplatelet extensions are again notably shorter (Figure 5A-B). As yet another control for specificity, Rab7T22N, which is known to disrupt late endocytic membrane traffic,<sup>23,47</sup> causes a trivial decline (from 17% to 13%) in the proportion of MKs that elaborate proplatelets (Figure 5A) and it does not truncate the cytoplasmic extensions (data not shown).

These results directly implicate a Rab27 protein in the efficiency and manner in which mature MKs fragment to release platelets, although the design of the dominant-negative constructs precludes reliable distinction between the a and b isoforms. However, the relative abundance of Rab27b, its considerable increase with MK differentiation, and its selective loss in the absence of NF-E2 combine to suggest that it is the more relevant factor in thrombopoiesis.

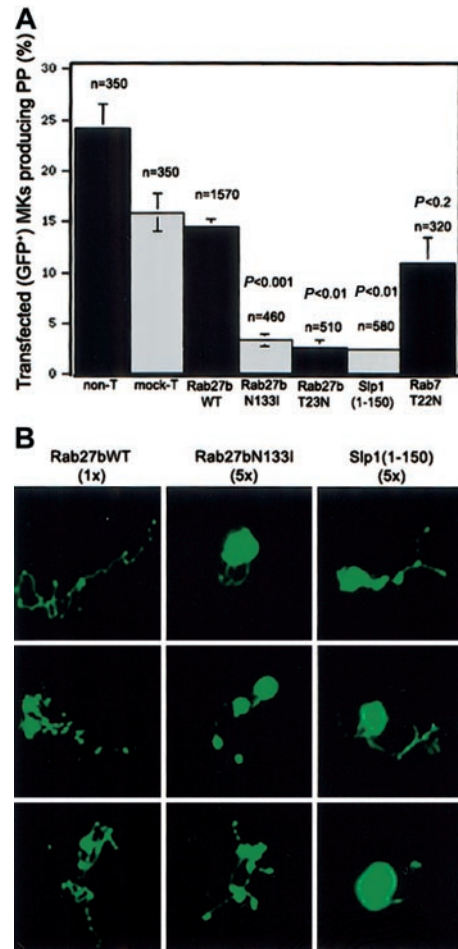


**Figure 5. Transient overexpression of dominant-negative Rab27b mutants, including an Slp1 fragment, results in reduced numbers and length of proplatelet extensions.** (A) Quantitative analysis of proplatelet formation (PPF) by fluorescence microscopy 18 to 24 hours following transfection of cultured (day 2.5) primary wild-type MKs using a biolistic "gene-gun" method. The first 2 bars indicate the frequency of PPF among untransfected and mock-transfected MKs under the experimental conditions. There is about a 5-fold decrease in PPF by MKs expressing GFP-tagged Rab27bN133I, Rab27bT23N, or Slp1 (1-150) compared with those expressing wild-type Rab27b. In contrast, MKs expressing GFP-Rab7T22N show a trivial and statistically insignificant decline in PPF. The number of GFP<sup>+</sup> cells scored for each construct and the statistical significance (Student *t* test) of the numeric differences between wild-type (WT) and dominant-negative samples are indicated above the histogram bars. Data (shown as mean ± SD) are pooled from 3 to 6 independent experiments (for the different constructs), which gave consistent results. (B) Representative fluorescence micrographs (original magnification, × 200) of proplatelet-forming MKs reveal the significant shortening of proplatelet shafts in cells expressing GFP-tagged Rab27bN133I or Slp1(1-150). Cells transfected with the wild-type or dominant inhibitory constructs are deliberately shown at different magnifications (original magnifications × 1 vs × 5) to highlight the appearance of proplatelets observed in each case.

#### Role for Rab27b in platelet-specific granules

To investigate potential sites and mode of action, we considered Rab27b in the light of established roles for other Rab proteins, which mediate various aspects of organelle synthesis and transport.<sup>14</sup> The Rab27b-specific antiserum R27B1 stains primary MKs in a granular pattern throughout the cell body (Figure 6A) and in proplatelets (Figure 6B). Costaining with β1 tubulin antiserum (Figure 6C), which highlights proplatelet shafts and the nascent marginal microtubule band,<sup>32</sup> shows that Rab27b is not associated exclusively with the thick microtubule bundles that line proplatelets; however, the granules containing Rab27b could certainly associate with other less abundant cellular microtubule forms that

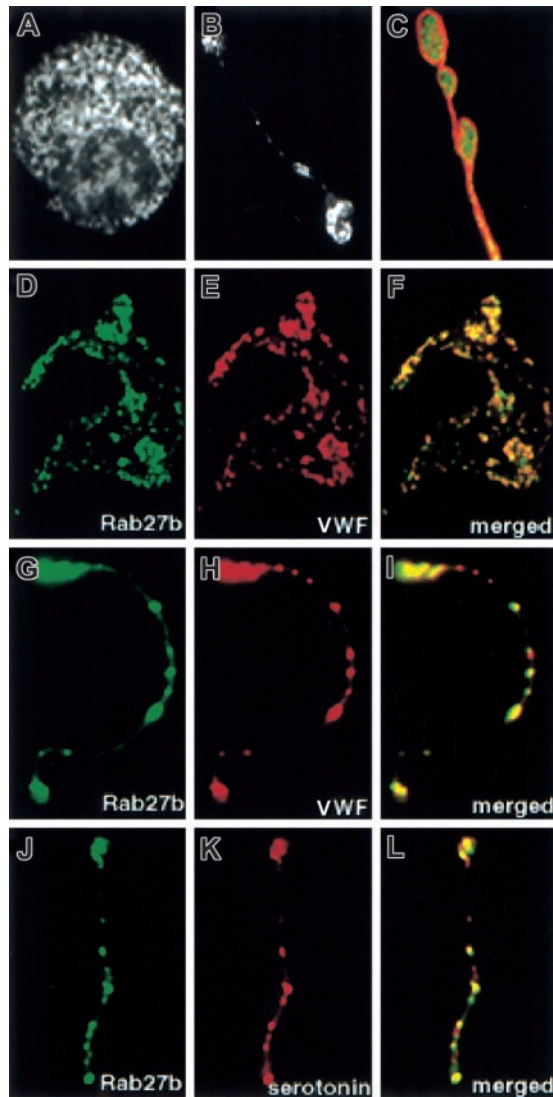


**Figure 6. Colocalization of Rab27b with  $\alpha$  and dense granules in MKs.** (A-B) Immunolocalization of Rab27b in the MK cell body (A) and in proplatelet extensions (B). Staining is granular in both sites. MKs were cytocentrifuged onto glass slides, fixed, and stained with the Rab27b-specific R27B1 antibody, followed by FITC-conjugated goat antirabbit IgG. (C) Rab27b is not exclusively associated with the lineage-specific thick marginal microtubule cytoskeleton, as revealed by costaining with R27B1 and a mouse  $\beta$ -tubulin monoclonal antibody (detected using Texas Red-conjugated donkey antimouse IgG). (D-I) Colocalization of Rab27b with the  $\alpha$ -granule marker VWF in the cell body and in proplatelet shafts, as revealed through separate immunostaining for Rab27b (D,G; antibody directly conjugated to FITC), VWF (E,H; antibody directly conjugated to Texas Red), and merging of the images (F,I). (J-L) Colocalization of Rab27b with the dense-granule marker serotonin in proplatelets, as revealed through separate immunostaining for Rab27b (J), serotonin (K; rat antiserotonin detected using Texas Red-conjugated goat antirat IgG), and merging of the images (L). Original magnifications,  $\times 600$  (A, D-F); and  $\times 1000$  (B-C, G-L).

are not readily apparent in this experiment. To identify the cytoplasmic compartment in which Rab27b is present, we performed double immunolabeling and detected colocalization of Rab27b with the  $\alpha$ -granule protein von Willebrand factor (VWF; Figure 6D-I). Although most VWF-stained particles show Rab27b staining, some Rab27b-positive granules do not contain VWF. To account for all of the visible Rab27b immunostain in primary MKs, we performed double immunostaining with serotonin, a marker of platelet-dense bodies. Rab27b-stained granules also show bright staining for serotonin (Figure 6J-L). These results confirm a previous report that suggested that Rab27b is mainly localized in the limiting membranes of platelet-dense and  $\alpha$  granules.<sup>21</sup>

Rab27a is implicated in actin-mediated intracellular capture of melanosomes,<sup>45,46</sup> but the abundance of actin fibers in mature MKs precludes meaningful assessment of physical associations between Rab27b and actin filaments. Rab27b may nevertheless function in aspects of granule assembly or transport. Indeed, plasma VWF levels are elevated in *gm/gm* mice, suggesting that excess VWF accumulates in the MK cytoplasm because its delivery to  $\alpha$  granules is impaired.<sup>10</sup> To address the possibility that Rab27 may operate to deliver protein cargo to developing platelet granules, we expressed the dominant Rab27b inhibitors T23N, N133I, and Slp1(1-150) in cultured MKs and examined the effects on VWF localization and abundance. All mutant forms fail to alter either the distribution or amount of VWF, which is abundantly expressed in cytoplasmic granules (Figure 7). Thus, Rab27 proteins appear not to be required for transport of  $\alpha$ -granule proteins to their organelle destination in maturing MKs.

## Discussion

This study presents evidence from normal MKs and independent mouse models of thrombocytopenia that point to the Rab27 subfamily as a component of the thrombopoietic machinery. We show that the cellular basis for thrombocytopenia in *gm/gm* mice is a profoundly compromised capacity to elaborate proplatelets, a

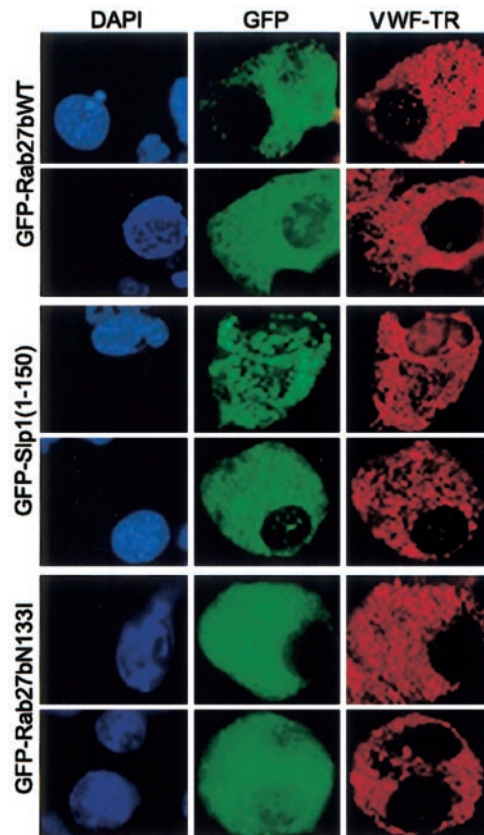


**Figure 7. Immunofluorescent localization of VWF in primary MKs transfected with wild-type or dominant-negative versions of Rab27.** There is no change in the distribution or abundance of VWF in MKs expressing GFP-tagged wild-type (WT,  $n = 50$ ) or dominant-negative forms Rab27bN133I ( $n = 54$ ) or Slp1(1-150) ( $n = 40$ ). MKs were transfected with GFP fusion constructs and harvested 24 hours later, cytocentrifuged onto glass slides, fixed, immunostained for VWF, and scored individually. Cells were mounted with aqueous medium containing DAPI (4,6 diamidino-2-phenylindole) and visualized by fluorescence microscopy. Original magnifications,  $\times 400$  for all panels.



phenotype shared with mice lacking the transcription factor NF-E2. Rab27b is an especially abundant platelet protein that is inactive or absent in MKs derived from *gm/gm* and p45 NF-E2<sup>-/-</sup> mice, respectively, and coats  $\alpha$  and dense granules, 2 secretory organelles with important roles in hemostasis. Expression of dominant-interfering Rab27 forms in primary MKs results in a substantial decline in proplatelet-forming cells, with concurrent reduction in the length of cytoplasmic extensions. These findings recapitulate the morphologic defects seen in *gm/gm* MKs and directly implicate a Rab27 protein in the initiation and subsequent elaboration of cytoplasmic processes en route to platelet release. Our results add to the growing appreciation of molecular mechanisms that govern the remarkable process by which a single MK fragments to produce thousands of blood platelets.

Although our studies focus on Rab27b, the dominant-negative strategy in itself does not distinguish between the individual roles of Rab27a and Rab27b. This is because the N133I and T23N mutants and Slp1 fragment likely sequester factors required for the action of both the a and b isoforms.<sup>45</sup> Nevertheless, the weight of evidence is more consistent with a special role for Rab27b in thrombopoiesis. *Ashen* mutant mice, which lack Rab27a,<sup>34</sup> do not have a defect in platelet production per se. Furthermore, among the small number of platelet-expressed Rab proteins, Rab27b expression increases the most with terminal MK differentiation and appears to be under the transcriptional regulation of NF-E2. Thus, though our experiments that directly test Rab27 function do leave open the possibility of some role for Rab27a in platelet biogenesis, between these 2 factors Rab27b is more likely the principal effector molecule. Based on their nonoverlapping patterns of expression<sup>21</sup> and identification of a large family of Rab27 effector proteins,<sup>45,46</sup> there is also the potential for unique functions for the a and b forms.

Addressing these and related questions presents a significant experimental challenge because proplatelet dynamics can only be studied in primary MKs, which resist conventional means of manipulating gene expression. We expressed plasmids in cultured MKs using a method for bombarding cells with DNA-coated gold particles.<sup>30,48</sup> This enables transgene expression in postmitotic MKs without significant toxic effects on proplatelet formation but transduction efficiencies are poor, and rigorous analysis relies on the ability to identify the fraction of cells with demonstrable transgene expression. Although the results are reproducible and meaningful, there are limits on the extent to which cellular detail can be resolved so that any role for Rabs in regulating the internal MK demarcation membrane system, for example, remains obscure. Despite these limitations, our data establish Rab27b as an important target of RGGT deficiency and of NF-E2 regulation and as a likely essential differentiation product in maturing MKs.

The size and complexity of the Rab protein family would suggest that any single member probably makes an individually small contribution toward the totality of organelle dynamics, although that contribution may be measurable and important. Our findings implicate Rab27b as only one component of key intracellular events and help define its role within NF-E2-dependent pathways of MK differentiation. Regarded in the context of the limited phenotype in *gunmetal* mice, our results reinforce the notion that properties limited to the Rab27 subfamily and a few other Rabs may render them especially sensitive to reduced RGGT enzyme levels.<sup>20</sup>

Transcriptional targets of NF-E2 must serve essential roles in molecular mechanisms of platelet biogenesis and release.<sup>5,36,49</sup> Some pathways that seem to function downstream of NF-E2, such

as prostaglandin metabolism<sup>37,50</sup> and inside-out integrin signaling,<sup>38,39</sup> are as yet not directly implicated in proplatelet formation or platelet release, although  $\beta$ 1 tubulin is both down-regulated in NF-E2-null MKs<sup>32</sup> and required for optimal platelet production.<sup>51</sup> Here we identify *Rab27b* as a new component in NF-E2-dependent pathways of platelet assembly. Like  $\beta$ 1 tubulin, Rab27b is lost in the absence of NF-E2 function and, acting alone or in combination with Rab27a, it appears to be essential for proplatelet formation. NF-E2 is recruited to candidate *cis*-elements in the *Rab27b* gene, which is therefore likely a bona fide transcriptional target. These findings support the idea that NF-E2 regulates many aspects of thrombopoiesis and that identification of NF-E2 target genes will continue to help elucidate underlying mechanisms. However, the apparent complexity of the pathways regulated, directly or indirectly, by NF-E2 precludes proving the requirement for individual components by introducing single genes in NF-E2-null MKs because this strategy is unlikely to rescue the discernible cellular defects.<sup>32</sup>

In contrast to our demonstration of physical association between p45 NF-E2 and the *Rab27B* gene locus using ChIP (Figure 4), we do not detect binding of the NF-E2 complex to a synthetic consensus oligonucleotide by a shift in electrophoretic mobility (data not shown). This would suggest that the purported interactions are weak or transient and acquire strength or stability mainly in the context of intact nuclear chromatin. The biology of NF-E2 is complicated, as cells modulate the relative abundance of alternative activating and repressive complexes precisely<sup>49</sup>; studies that implicate it in transcriptional regulatory functions in vitro or in transgenic mice<sup>40,42,44,52-54</sup> are not accurately reflected in knockout mice,<sup>55-58</sup> and discrepancies are noted in roles defined in different assays.<sup>43,59,60</sup> NF-E2 is also subject to influential posttranslational modifications.<sup>61,62</sup> The present observations are consistent with its likely complex role in regulating *Rab27B* gene expression in MKs. Future promoter studies might define the degree to which NF-E2 regulates this gene directly.

The simplest interpretation of our findings also sheds new light on mechanisms of proplatelet formation. Rab27b is prominently found in association with 2 platelet-specific organelles,  $\alpha$  and dense granules, yet dominant-interfering constructs do not alter the granular staining distribution or abundance of VWF. This at least suggests that a Rab27 protein is not required to deliver VWF from the *trans*-Golgi network to developing  $\alpha$  granules; instead, Rab27 function is essential for elaboration of normal proplatelets. Accordingly, our results would suggest that proplatelet formation relies critically on platelet granules expressing differentiation-related effector molecules and that proplatelet formation is coupled in previously unsuspected ways to signals, like Rab27b, that reside on granule surfaces. Platelet release represents the culmination of MK maturation but probably requires cell-intrinsic cues and mechanisms for its onset and execution. Rab27b may serve to link  $\alpha$  and/or dense granules with signals that drive proplatelet formation.

Such a model does not exclude an independent or related role for Rab27b in transporting granules along proplatelets. Other Rab proteins function in this capacity,<sup>63-65</sup> and Rab27b colocalizes with platelet granules in both the cell body and proplatelet extensions. Indeed, Rab27b function may be considered in light of the role of its closest relative, Rab27a, in melanocytes. Here, melanosomes initially move along microtubules in a Rab27-independent manner. In the cell periphery, melanosome-associated Rab27a recruits melanophilin, a postulated effector molecule that facilitates association of melanosomes with actin filaments.<sup>24,45,46,66</sup> There are several

known Rab27 effectors and distinct mechanisms impart selective effects in different cell types.<sup>45,46,66</sup> By analogy, platelet granule-associated Rab27b might help capture proteins that operate within the actin cytoskeleton. Growth and extension of proplatelets requires repeated branching, which is dependent on actin,<sup>4</sup> but the relative roles of actin and microtubules in proplatelet organelle transport are not known. Our data imply that some aspects of granule transport and proplatelet extension are intricately coupled, and the potential role of actin filaments in that coupling merits further investigation.

## References

1. Becker RP, de Bruyn PP. The transmural passage of blood cells into myeloid sinusoids and the entry of platelets into the sinusoidal circulation: a scanning electron microscopic investigation. *Am J Anat.* 1976;145:183-205.
2. Scurfield G, Radley JM. Aspects of platelet formation and release. *Am J Hematol.* 1981;10:285-296.
3. Choi ES, Nichol JL, Hokom MM, Hornkohl AC, Hunt P. Platelets generated in vitro from proplatelet-displaying human megakaryocytes are functional. *Blood.* 1995;85:402-413.
4. Italiano JE, Lecine P, Shivdasani RA, Hartwig JH. Blood platelets are assembled principally at the ends of proplatelet processes produced by differentiated megakaryocytes. *J Cell Biol.* 1999;147:1299-1312.
5. Shivdasani RA, Rosenblatt MF, Zucker-Franklin D, et al. Transcription factor NF-E2 is required for platelet formation independent of the actions of thrombopoietin/MGDF in megakaryocyte development. *Cell.* 1995;81:695-704.
6. Shivdasani RA, Fujiwara Y, McDevitt MA, Orkin SH. A lineage-selective knockout establishes the critical role of transcription factor GATA-1 in megakaryocyte growth and platelet development. *EMBO J.* 1997;16:3965-3973.
7. Swank RT, Novak EK, McGarry MP, et al. Abnormal vesicular trafficking in mouse models of Hermansky-Pudlak syndrome. *Pigment Cell Res.* 2000;13:59-67.
8. Dell'Angelica EC, Shotelersuk V, Aguilar RC, Gahl WA, Bonifacio JS. Altered trafficking of lysosomal proteins in Hermansky-Pudlak syndrome due to mutations in the beta 3A subunit of the AP-3 adaptor. *Mol Cell.* 1999;3:11-21.
9. Huang L, Kuo YM, Gitschier J. The pallid gene encodes a novel, syntaxin 13-interacting protein involved in platelet storage pool deficiency. *Nat Genet.* 1999;23:329-332.
10. Swank RT, Jiang SY, Reddington M, et al. Inherited abnormalities in platelet organelles and platelet formation and associated altered expression of low molecular weight guanosine triphosphate-binding proteins in the mouse pigment mutant gunmetal. *Blood.* 1993;81:2626-2635.
11. Novak EK, Reddington M, Zhen L, et al. Inherited thrombocytopenia caused by reduced platelet production in mice with the gunmetal pigment gene mutation. *Blood.* 1995;85:1781-1789.
12. Detter JC, Zhang Q, Mules EH, et al. Rab geranyltransferase alpha mutation in the gunmetal mouse reduces Rab prenylation and platelet synthesis. *Proc Natl Acad Sci U S A.* 2000;97:4144-4149.
13. Pereira-Leal JB, Hume AN, Seabra MC. Prenylation of Rab GTPases: molecular mechanisms and involvement in genetic disease. *FEBS Lett.* 2001;498:197-200.
14. Zerial M, McBride H. Rab proteins as membrane organizers. *Nat Rev Mol Cell Biol.* 2001;2:107-117.
15. Seabra MC, Mules EH, Hume AN. Rab GTPases, intracellular traffic and disease. *Trends Mol Med.* 2002;8:23-30.
16. Zhang Q, Zhen L, Li W, et al. Cell-specific abnormal prenylation of Rab proteins in platelets and melanocytes of the gunmetal mouse. *Br J Haematol.* 2002;117:414-423.
17. Chen D, Guo J, Miki T, Tachibana M, Gahl WA. Molecular cloning and characterization of rab27a and rab27b, novel human rab proteins shared by melanocytes and platelets. *Biochem Mol Med.* 1997;60:27-37.
18. Ramalho JS, Tolmachova T, Hume AN, et al. Chromosomal mapping, gene structure and characterization of the human and murine RAB27B gene. *BMC Genet.* 2001;2:2.
19. Nagata K, Itoh H, Katada T, et al. Purification, identification, and characterization of two GTP-binding proteins with molecular weights of 25,000 and 21,000 in human platelet cytosol: one is the rap1/smg21/Krev-1 protein and the other is a novel GTP-binding protein. *J Biol Chem.* 1989;264:17000-17005.
20. Seabra MC, Ho YK, Anant JS. Deficient geranylgeranylation of Ram/Rab27 in choroideremia. *J Biol Chem.* 1995;270:24420-24427.
21. Barral DC, Ramalho JS, Anders R, et al. Functional redundancy of Rab27 proteins and the pathogenesis of Griscelli syndrome. *J Clin Invest.* 2002;110:247-257.
22. Zhao S, Torii S, Yokota-Hashimoto H, Takeuchi T, Izumi T. Involvement of Rab27b in the regulated secretion of pituitary hormones. *Endocrinology.* 2002;143:1817-1824.
23. Feng Y, Press B, Wandinger-Ness A. Rab 7: an important regulator of late endocytic membrane traffic. *J Cell Biol.* 1995;131:1435-1452.
24. Hume AN, Collinson LM, Rapak A, Gomes AQ, Hopkins CR, Seabra MC. Rab27a regulates the peripheral distribution of melanosomes in melanocytes. *J Cell Biol.* 2001;152:795-808.
25. Lecine P, Blank V, Shivdasani R. Characterization of the hematopoietic transcription factor NF-E2 in primary murine megakaryocytes. *J Biol Chem.* 1998;273:7572-7578.
26. Lewis SA, Gu W, Cowan NJ. Free intermingling of mammalian b-tubulin isotypes among functionally distinct microtubules. *Cell.* 1987;49:539-548.
27. McDonald TP, Jackson CW. Thrombopoietin derived from human embryonic kidney cells stimulates an increase in DNA content of murine megakaryocytes in vivo. *Exp Hematol.* 1990;18:758-763.
28. Forsberg EC, Downs KM, Christensen HM, Im H, Nuzzi PA, Bresnick EH. Developmentally dynamic histone acetylation pattern of a tissue-specific chromatin domain. *Proc Natl Acad Sci U S A.* 2000;97:14494-14499.
29. Harlow E, Lane D. *Antibodies: A Laboratory Manual.* Cold Spring Harbor, NY: Cold Spring Harbor Laboratory; 1988.
30. Sanford JC, Smith FD, Russell JA. Optimizing the biolistic process for different biological applications. *Methods Enzymol.* 1993;217:483-509.
31. Lecine P, Villeval J-L, Vyas P, Swencki B, Xu Y, Shivdasani RA. Mice lacking transcription factor NF-E2 validate the proplatelet model of thrombopoiesis and show a platelet production defect that is intrinsic to megakaryocytes. *Blood.* 1998;92:1608-1616.
32. Lecine P, Italiano JE Jr, Kim SW, Villeval JL, Shivdasani RA. Hematopoietic-specific beta 1 tubulin participates in a pathway of platelet biogenesis dependent on the transcription factor NF-E2. *Blood.* 2000;96:1366-1373.
33. Stinchcombe JC, Barral DC, Mules EH, et al. Rab27a is required for regulated secretion in cytotoxic T lymphocytes. *J Cell Biol.* 2001;152:825-834.
34. Wilson SM, Yip R, Swing DA, et al. A mutation in Rab27a causes the vesicle transport defects observed in ashen mice. *Proc Natl Acad Sci U S A.* 2000;97:7933-7938.
35. Shirakawa R, Yoshioka A, Horiuchi H, Nishioka H, Tabuchi A, Kita T. Small GTPase Rab4 regulates Ca<sup>2+</sup>-induced alpha-granule secretion in platelets. *J Biol Chem.* 2000;275:33844-33849.
36. Onodera K, Shavit JA, Motohashi H, Yamamoto M, Engel JD. Perinatal synthetic lethality and hematopoietic defects in compound mafG::maff mutant mice. *EMBO J.* 2000;19:1335-1345.
37. Deveaux S, Cohen-Kaminsky S, Shivdasani RA, et al. p45 NF-E2 regulates the expression of thromboxane synthase in megakaryocytes. *EMBO J.* 1997;16:5654-5661.
38. Shiraga M, Ritchie A, Aidoudi S, et al. Primary megakaryocytes reveal a role for transcription factor NF-E2 in integrin alpha IIb beta 3 signaling. *J Cell Biol.* 1999;147:1419-1430.
39. Eto K, Murphy R, Kerrigan SW, et al. Megakaryocytes derived from embryonic stem cells implicate CalDAG-GEFI in integrin signaling. *Proc Natl Acad Sci U S A.* 2002;99:12819-12824.
40. Forsberg EC, Downs KM, Bresnick EH. Direct interaction of NF-E2 with hypersensitive site 2 of the beta-globin locus control region in living cells. *Blood.* 2000;96:334-339.
41. Wen SC, Roder K, Hu KY, et al. Loading of DNA-binding factors on an erythroid enhancer. *Mol Cell Biol.* 2000;20:1993-2003.
42. Ney PA, Sorrentino BP, McDonagh KT, Nienhuis AW. Tandem AP-1-binding sites within the human b-globin dominant control region function as an inducible enhancer in erythroid cells. *Genes Dev.* 1990;4:993-1006.
43. Armstrong JA, Emerson BM. NF-E2 disrupts chromatin structure at human beta-globin locus control region hypersensitive site 2 in vitro. *Mol Cell Biol.* 1996;16:5634-5644.
44. Gong QH, McDowell JC, Dean A. Essential role of NF-E2 in remodeling of chromatin structure and transcriptional activation of the epsilon-globin gene in vivo by 5' hypersensitive site 2 of the beta-globin locus control region. *Mol Cell Biol.* 1996;16:6055-6064.
45. Strom M, Hume AN, Tarafder AK, Barkagianni E, Seabra MC. A family of Rab27-binding proteins: melanophilin links Rab27a and myosin Va function in melanosome transport. *J Biol Chem.* 2002;277:25423-25430.
46. Fukuda M, Kuroda TS, Mikoshiba K. Slac2-a/

- melanophilin, the missing link between Rab27 and myosin Va: implications of a tripartite protein complex for melanosome transport. *J Biol Chem.* 2002;277:12432-12436.
47. Vitelli R, Santillo M, Lattero D, et al. Role of the small GTPase Rab7 in the late endocytic pathway. *J Biol Chem.* 1997;272:4391-4397.
  48. Johnston SA, Anziano PQ, Shark K, Sanford JC, Butow RA. Mitochondrial transformation in yeast by bombardment with microprojectiles. *Science.* 1988;240:1538-1541.
  49. Motohashi H, Katsuoka F, Shavit JA, Engel JD, Yamamoto M. Positive or negative MARE-dependent transcriptional regulation is determined by the abundance of small Maf proteins. *Cell.* 2000;103:865-875.
  50. Yaekashiwa M, Wang LH. Transcriptional control of the human thromboxane synthase gene in vivo and in vitro. *J Biol Chem.* 2002;277:22497-22508.
  51. Schwer HD, Lecine P, Tiwari S, Italiano JE, Hartwig JH, Shivdasani RA. A lineage-restricted and divergent beta-tubulin isoform is essential for the biogenesis, structure and function of blood platelets. *Curr Biol.* 2001;11:579-586.
  52. Talbot D, Grosveld F. The 5' HS 2 of the globin locus control region enhances transcription through the interaction of a multimeric complex binding at two functionally distinct NF-E2 binding sites. *EMBO J.* 1991;10:1391-1398.
  53. Kotkow KJ, Orkin SH. Dependence of globin gene expression in mouse erythroleukemia cells on the NF-E2 heterodimer. *Mol Cell Biol.* 1995;15:4640-4647.
  54. Stamatoyannopoulos JA, Goodwin A, Joyce T, Lowrey CH. NF-E2 and GATA binding motifs are required for the formation of DNase I hypersensitive site 4 of the human b-globin locus control region. *EMBO J.* 1995;14:106-115.
  55. Shivdasani RA, Orkin SH. Erythropoiesis and globin gene expression in mice lacking the transcription factor NF-E2. *Proc Natl Acad Sci U S A.* 1995;92:8690-8694.
  56. Fiering S, Epner E, Robinson K, et al. Targeted deletion of 5'HS2 of the murine b-globin LCR reveals that it is not essential for proper regulation of the b-globin locus. *Genes Dev.* 1995;9:2203-2213.
  57. Martin F, van Deursen JM, Shivdasani RA, Jackson CW, Troutman AG, Ney PA. Erythroid maturation and globin gene expression in mice with combined deficiency of NF-E2 and nrf-2. *Blood.* 1998;91:3459-3466.
  58. Kuroha T, Takahashi S, Komeno T, Itoh K, Nagasawa T, Yamamoto M. Ablation of Nrf2 function does not increase the erythroid or megakaryocytic cell lineage dysfunction caused by p45 NF-E2 gene disruption. *J Biochem (Tokyo).* 1998;123:376-379.
  59. Goodwin AJ, McInerney JM, Glander MA, Pomerantz O, Lowrey CH. In vivo formation of a human beta-globin locus control region core element requires binding sites for multiple factors including GATA-1, NF-E2, erythroid Kruppel-like factor, and Sp1. *J Biol Chem.* 2001;276:26883-26892.
  60. Sawado T, Igarashi K, Groudine M. Activation of beta-major globin gene transcription is associated with recruitment of NF-E2 to the beta-globin LCR and gene promoter. *Proc Natl Acad Sci U S A.* 2001;98:10226-10231.
  61. Garingo AD, Suhasini M, Andrews NC, Pilz RB. cAMP-dependent protein kinase is necessary for increased NF-E2 DNA complex formation during erythroleukemia cell differentiation. *J Biol Chem.* 1995;270:9169-9177.
  62. Hung HL, Kim AY, Hong W, Rakowski C, Blobel GA. Stimulation of NF-E2 DNA binding by CREB-binding protein (CBP)-mediated acetylation. *J Biol Chem.* 2001;276:10715-10721.
  63. Pfeffer SR. Rab GTPases: specifying and deciphering organelle identity and function. *Trends Cell Biol.* 2001;11:487-491.
  64. Hammer JA, Wu XS. Rabs grab motors: defining the connections between Rab GTPases and motor proteins. *Curr Opin Cell Biol.* 2002;14:69-75.
  65. Smythe E. Direct interactions between rab GTPases and cargo. *Mol Cell.* 2002;9:205-206.
  66. Wu XS, Rao K, Zhang H, et al. Identification of an organelle receptor for myosin-Va. *Nat Cell Biol.* 2002;4:271-278.